Chemosphere 314 (2023) 137675

Contents lists available at ScienceDirect

Chemosphere

journal homepage: www.elsevier.com/locate/chemosphere

The role of biomass elemental composition and ion-exchange in metal sorption by algae

Ana R.F. Carreira [a], Telma Veloso [a,b], Inês P.E. Macário [a,b], Joana L. Pereira [a,b], Sónia P.M. Ventura [a], Helena Passos [a,*], João A.P. Coutinho [a]

[a] CICECO - Aveiro Institute of Materials, Department of Chemistry, University of Aveiro, 3810-193, Aveiro, Portugal
[b] Department of Biology & CESAM, University of Aveiro, Aveiro, Portugal

HIGHLIGHTS

- Eleven biomass samples were evaluated for metal sorption in quaternary systems.
- Brown macroalgae achieved the best metal sorption capacity.
- All biomass were selective for Cu^{2+}, with carboxyl groups being relevant for sorption.
- Biomass with higher carbon, nitrogen and hydrogen (%) have lower sorption capacity.
- Ion-exchange was identified as the main metal sorption mechanism.

GRAPHICAL ABSTRACT

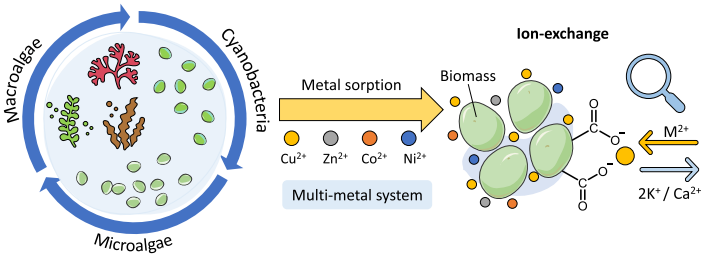

ARTICLE INFO

Handling Editor: A ADALBERTO NOYOLA

Keywords:
Macroalgae
Microalgae
Cyanobacteria
Screening
Sorption mechanism
Metal recovery

ABSTRACT

The use of macroalgae, microalgae and cyanobacteria for metal sorption has been widely reported. Still, there are no studies allowing a direct comparison of the performance of these biomasses, especially while evaluating metal competition. The simultaneous sorption of Co^{2+}, Cu^{2+}, Ni^{2+} and Zn^{2+} present in a multi-elemental solution by six macroalgae, two microalgae and three cyanobacteria was evaluated. Brown macroalgae were shown to be the most promising biosorbent, with *Undaria pinnatifida* having a total metal sorption capacity of 0.6 mmol g^{-1}. Overall, macroalgae performed better than microalgae, followed by cyanobacteria. Carboxyl groups were identified as being the main functional groups involved in metal sorption, and all biomass samples were found to be selective to Cu^{2+}. This was linked not only to its higher complexation constant value with relevant functional groups when compared to the remaining metals, but also the Irving-Williams series. The release of K^{+} and Ca^{2+} to the aqueous solution during the metal sorption was followed. The obtained results suggest they are readily exchanged with metals in the solution, indicating the occurrence of an ion-exchange mechanism in metal sorption by most biomass. Red macroalgae are an exception to the reported trends, suggesting that their metal sorption mechanism may differ from the other biomass types.

* Corresponding author.
E-mail address: hpassos@ua.pt (H. Passos).

https://doi.org/10.1016/j.chemosphere.2022.137675
Received 14 September 2022; Received in revised form 17 November 2022; Accepted 25 December 2022
Available online 29 December 2022

1. Introduction

The strong dependence of modern societies on metal-rich commodities is putting pressure on natural metal reserves (LI and feng CAI, 2021). To avoid short-term supply and demand constraints, the metal industry must pursue a shift from a linear to a circular economy. Wastewaters such as industrial, agricultural and municipal effluents are produced in large volumes and could be viable secondary metal sources (Nobahar et al., 2022; Millán-Becerro et al., 2022; Dutta et al., 2021). Wastewaters have an inherent organic and inorganic heterogeneity which adds complexity to these matrices. Recovering metals from wastewater can be achieved using processes such as hydrometallurgy, electrodeposition, membranes, bioleaching, chemical precipitation and (bio)sorption (Dutta et al., 2021). Hybrid methodologies can also be developed by combining different processes for better efficiency (Dolker and Pant, 2019; Birloaga and Vegliò, 2022). However, some of these processes are energy and/or solvent-intensive, increasing the overall costs of the process while producing substantial waste volumes.

Biosorption can be a sustainable and cost-effective approach for recovering metals from wastewater (Dodbiba et al., 2015). Herein, biosorption is defined as the passive interaction of the biomass surface with metal ions. Biosorption can occur in living and non-living biomass. The use of non-living biomass for metal sorption has several advantages such as good cost-effectiveness, application in wider pH and metal concentration ranges, no need for additional nutrients and facilitated metal recovery compared to intra-cellular metal accumulation (Salam, 2019). Non-living biomass can afford quicker and more efficient metal sorption than living biomass (Lin et al., 2020), also bearing advantages such as control over proliferation and potential fouling events. The success of metal sorption depends on the initial metal concentration, contact time, pH, metal:sorbent ratio and the presence of competing ions (Shaaban et al., 2017; Kamarudzaman et al., 2022). Optimization of the sorption process also depends on understanding the underlying mechanisms of metal sorption. Some of the mechanisms involved in metal sorption include physical sorption, chemical sorption and ion-exchange (Escudero-Oñate and Villaescusa, 2018; Akpomie et al., 2015; Javanbakht et al., 2014). The mechanism(s) involved in metal sorption will also depend on the composition of the used biomass.

Several biomass matrices have been successfully employed for metal sorption, including fruit waste (Wang et al., 2022), nuts (Kayranli et al., 2022), spent mushrooms (Kamarudzaman et al., 2022), coffee husk derivatives (thi Quyen et al., 2021), and seeds (Sheikh et al., 2021). Macroalgae, microalgae (Ibrahim et al., 2018; Romera et al., 2007) and cyanobacteria (Gahlout et al., 2017) have also been widely studied for metal sorption, due to their bioavailability, biodegradability, low-cost and efficiency (Lin et al., 2020; Yadav et al., 2021). The invasive character of some algae also makes their removal environmentally beneficial. Metal sorption on non-living organisms is related to their cell wall constitution. Metal interaction will mainly occur *via* the functional groups present in the cell wall – carboxyl, hydroxyl, thiol, amino and phosphate groups – and their abundance and availability will determine the success of biosorption (Kanamarlapudi et al., 2018). Efforts have been made to find effective biosorbents, with studies comparing the metal sorption efficiency of different macroalgae (Romera et al., 2007; Wang and Chen, 2009; Pennesi et al., 2012) and, to a lesser extent, evaluating the efficiency of macroalgae *vs* microalgae (Piccini et al., 2018) and microalgae *vs* cyanobacteria (Inthorn et al., 2002). Still, a simultaneous comparison of macroalgae, microalgae and cyanobacteria under the same experimental conditions seems to be lacking.

Algae and cyanobacteria are usually used for water decontamination in general rather than specifically for metal recovery (Blanco-Vieites et al., 2022). This causes some divergences in the optimization of metal sorption. Water decontamination seeks the complete removal of metal from the wastewater, often resulting in the addition of high biomass amounts for low metal concentrations (Ibrahim et al., 2018; Ajjabi and Chouba, 2009). In contrast, using biosorption for metal recovery aims at the saturation of the functional groups of the biomass, requiring a good equilibrium between biomass dosage and metal concentration to ensure optimal metal pre-concentration. The selection of target metals and their concentration also depends on the end goal. In water decontamination, it is common to study low metal concentrations, sometimes close to the drinking water and wastewater limits (Costa et al., 2020), with target metals being selected due to their toxicity rather than their criticality and economical value (Znad et al., 2022). Studies using sorption for metal recovery tend to focus on aqueous solutions with higher metal concentrations and rich in critical or valuable metals, such as acid mine drainage wastewaters (Ramasamy et al., 2019). Overall, there is a lack of reports focusing on the use of algae and cyanobacteria as metal pre-concentrators, but also a dearth of studies conducted on multi-elemental metal solutions (Ramasamy et al., 2019; Bina et al., 2006). Most biosorption studies are based on aqueous solutions of a single metal, disregarding the ion competition effect (Ibrahim et al., 2018; Romera et al., 2007; Ramasamy et al., 2019; Bina et al., 2006). For metal recovery purposes, it is important to consider metal competition since wastewaters are generally composed of several metals.

Herein, a direct comparison of macroalgae, microalgae and cyanobacteria performance is enabled while considering the metal competition effect. Eight algae (six macro- and two microalgae) and three cyanobacteria were screened for metal sorption in multi-elemental aqueous solutions. The metals Co^{2+}, Cu^{2+}, Ni^{2+} and Zn^{2+} were selected due to their significance for developing low-carbon technology, criticality and their equal valency (Christmann and Lefebvre, 2022; Miyamoto et al., 2019; Watari et al., 2020). All biomass samples were characterized through Fourier transform infrared (FTIR), elemental analysis and total reflection X-ray fluorescence spectrometer (TXRF). The correlation between the biomass composition (carbon, hydrogen, nitrogen, sulfur, oxygen, and ash content percents) and sorption capacity was evaluated. The release of Ca^{2+} and K^{+} ions from the biomass to the aqueous solution was studied to understand the underlying sorption mechanism better.

2. Materials and methods

All chemicals were purchased and used as received. $CoSO_4{\cdot}7H_2O$ (>99 wt %), $CuSO_4{\cdot}5H_2O$ (>99 wt %) and $ZnSO_4{\cdot}7H_2O$ (>99 wt %) were obtained from Merck. $NiSO_4{\cdot}6H_2O$ (>99 wt %) was purchased from Riedel de Haen. Yttrium standard (1000 mg L^{-1} of Y(III) in 2 wt % nitric acid), poly(vinyl alcohol) (>99 wt %) and Triton® X-100 (for analysis) were purchased from Sigma Aldrich. All solutions were prepared in ultra-pure water which was obtained through a Millipore filter system MilliQ®. All metal solutions were prepared by gravimetrically weighing ($\pm 10^{-4}$ g) the correct amount of each metal salt. The glass material was previously washed with nitric acid (20 v/v %) purchased from Merck (65 wt %) and further rinsed with ultra-pure water.

2.1. Biomass collection and pre-treatment

Six macroalgae (*Gracilaria* sp., *Gelidium* sp., *Sargassum* sp., *Saccharina latissima, Ulva rigida and Undaria pinnatifida*), two microalgae (*Isochrysis galbana* and *Phaeodactylum tricornutum*) and three cyanobacteria (*Anabaena cylindrica* PCC 7122, *Nostoc muscorum* UTAD_N213 and *Spirulina* sp.) were screened for their metal sorption capacity. *U. rigida*, *Gracilaria* sp., *U. pinnatifida, Sargassum* sp. *and Gelidium* sp. were kindly provided by ALGAplus, Lda. *Gracilaria* sp. was received dry and ground while *U. rigida*, *U. pinnatifida* and *Sargassum* sp. were also received dry, but grinding was performed in the laboratory by freezing the biomass with liquid nitrogen and immediately grinding it with a domestic coffee grinder. The obtained particles were mechanically sieved to select particles with a size under 200 μm. *S. latissima* was kindly provided by Algaia SA (Saint Lo, France). *S. latissima* and *Gelidium* sp. were pre-dried before delivery and ground at lab scale as previously described. *I. galbana* and *P. tricornutum* were acquired dry at Necton S.A. and used

without further treatment. *Spirulina* sp. was purchased dry from Shine Superfoods – Alma & Valor and used as received. *A. cylindrica* PCC 7122 and *N. muscorum* UTAD_N213 were cultured in 5 L Schott Duran® glassware containing sterilized liquid Woods Hole culture medium (MBL) (Womersley, 1973), in an incubation chamber at (293 ± 2) K, under a 16:8 h light-dark photoperiod using 2300 lx from cool white fluorescent tubes. After 13 days in culture, the biomass was harvested and concentrated through centrifugation at 277 K and 4111 *g*. The fresh biomass was freeze-dried at < 150 mTorr resorting to a benchtop K, VirTis with a Vacuumbrand pump for one week. All biomass was kept in a dry and light-protected place at room temperature.

2.2. Biosorption batch studies

Since this work is focused on metal recovery, a fair metal:biomass ratio is required to achieve good metal pre-concentration. In mono-metallic assays with Cu^{2+}, Ni^{2+} and Zn^{2+}, promising results were achieved with an initial metal concentration of 50 ppm and 500 ppm of non-living algae (Romera et al., 2007). Since in multi-elemental assays the metal sorption efficiency is deemed to be lower than in mono-elemental assays, herein the total initial metal concentration was reduced to 40 ppm, with 10 ppm each of Cu^{2+}, Co^{2+}, Ni^{2+} and Zn^{2+} being simultaneously placed in contact with 500 ppm of algae. The pH of the solutions was adjusted to 4 by adding diluted sulfuric acid and determined using a Mettler Toledo SevenMultiTMdual pH meter (±0.02). At low pH values, there is competition between protons and metals for the available binding sites, which limits the metal sorption efficiency of the biomass (Zeraatkar et al., 2016). In contrast, at high pH values, metal precipitation may occur, once again hindering the metal sorption efficiency. Thus, performing the screening assay at pH = 4 is a reasonable compromise. The batch experiments were conducted in Schott Duran® glassware in an orbital shaker (IKA KS4000 ic control) at 200 rpm and (303 ± 1) K by adding 500 ppm of dried non-living biomass to each multi-elemental metal solution (100 mL). No biomass was added to the control which was simultaneously subjected to the same procedure as the samples. No metal loss was verified in the controls over time. Samples of sorbent suspension were collected (1.5 mL) after 6 and 24 h of contact, centrifuged for 2 min at 12,000 rpm and the liquid phase was separated from the residual biomass. All assays were conducted in triplicate.

2.3. Metal quantification

Metal quantification was performed by total reflection X-ray fluorescence spectrometry (TXRF) using a Picofox S2 (Bruker Nano (Billerica, MA, USA)) equipped with a molybdenum X-ray source. All the analyses were conducted at a 50 kV voltage and 600 μA current for 300 s. Quartz sample carriers were coated with 10 μL of silicon in isopropanol solution and dried at (353 ± 1) K for at least 15 min. A known amount of yttrium was added to each sample and 10 μL of this solution was added to a pre-treated quartz carrier and dried at (353 ± 1) K for at least 30 min.

The amount of metal *per* unit of biomass (sorption capacity, q, $mmol \cdot g^{-1}$) at time t was calculated according to Equation (1):

$$q = \frac{V\,(C_0 - C_t)}{m} \quad (1)$$

where V is the volume of the solution (L), C_0 ($mmol \cdot L^{-1}$) is the initial concentration of each metal, C_t ($mmol \cdot L^{-1}$) is the concentration of each metal at that time (t) and m is the biomass mass (g). The selectivity of the biomass was determined as shown in Equation (2):

$$S = \frac{q_{metal1}}{q_{metal2}} \quad (2)$$

where q_{metal1} ($mmol \cdot g^{-1}$) is the sorption capacity of a metal and q_{metal2} ($mmol \cdot g^{-1}$) is the sorption capacity of a second metal.

2.4. Biomass characterization

All the evaluated non-living biomass matrices were characterized *via* Fourier transform infrared (FTIR), elemental analysis and total reflection X-ray fluorescence spectrometry (TXRF). The FTIR spectra of biomass samples were acquired by a PerkinElmer Spectrum BX spectrometer with a diamond crystal and a horizontal Golden Gate attenuated total reflection (ATR) cell. Each sample was analyzed at wavenumbers ranging from 4000 to 400 cm^{-1}, with a resolution of 4 cm^{-1} and a total of 32 scans. While the FTIR of the biomass pre-sorption was acquired for all biomass samples the spectra after sorption were only acquired for the macroalgal *Sargassum* sp., the microalgal *P. tricornutum*) and the cyanobacterium (*Spirulina* sp.). The elemental analysis (C, H, N and S) of the biomass samples was obtained using the equipment LECO TruSpec series 630-200-200 (Michigan, US), whereas the oxygen content was determined by difference after ash content determination. The calcium and potassium content of all biomass matrices was evaluated *via* TXRF by suspending the biomass in a solution of 0.8 g of poly(vinyl alcohol) (1 wt %) and 0.2 g of Triton® X-100 (1 wt %), spiked with a known concentration of yttrium. The subsequent sample preparation was made as described in sub-section 2.3.

3. Results and discussion

The biomass screening included different macroalgae, microalgae and cyanobacteria to facilitate the simultaneous comparison of the metal sorption capacity of different biomass. This is usually done by comparing works conducted under different experimental conditions (Romera et al., 2007) and limited biomass diversity (Ibrahim et al., 2018; Fabre et al., 2021), which hinders the comparison of the sorption capacity of macroalgae, microalgae and cyanobacteria (Ibrahim et al., 2018; Romera et al., 2007; Fabre et al., 2021; Radway et al., 2001). A comprehensive screening was performed in multi-elemental metal solutions since metal recovery often involves complex matrices. All biomass samples were analyzed by elemental analysis and FTIR to better understand their composition. The presence of inorganic elements in the biomass structure was evaluated by TXRF. The release of ions such as Ca^{2+} and K^{+} during the sorption process was evaluated to better understand the mechanism behind metal sorption in the different biomass samples.

3.1. Screening assay

To evaluate the potential of different algal biomass samples for metal sorption, eleven samples were selected and placed in contact with a multi-elemental solution of Co^{2+}, Cu^{2+}, Ni^{2+} and Zn^{2+}, each with a concentration of 10 ppm and at pH = 4. After placing the biomass in contact with the metal solution, samples were collected at 6 and 24 h. No significant differences in the sorption capacity of the biomass were found across time (Fig. S1). The sorption capacity of each biomass after 6 h of contact is represented in Fig. 1.

Brown macroalgae afforded better metal sorption capacity values than the remaining biomass types, followed by the green macroalgae *U. rigida*. The red macroalgae showed the lowest sorption capacity within the macroalgae group. Similar tendencies were previously reported in mono-elemental sorption studies, with brown macroalgae being a more promising metal sorbent than green and red macroalgae (Wang and Chen, 2009; Pennesi et al., 2012). Brown macroalgae are rich in alginic acid and, therefore, display a large number of carboxyl and hydroxyl groups (Davis et al., 2003). This may justify their higher ability for metal sorption, especially at pH values close to the acid dissociation constant of carboxylic acids (pK_a 1.7–4.7) (Davis et al., 2003; Dean, 1999). Sheng et al. (2004) reported mono-elemental studies using dried non-living *Sargassum* sp., *Ulva* sp. and *Gracilaria* sp. for the sorption of

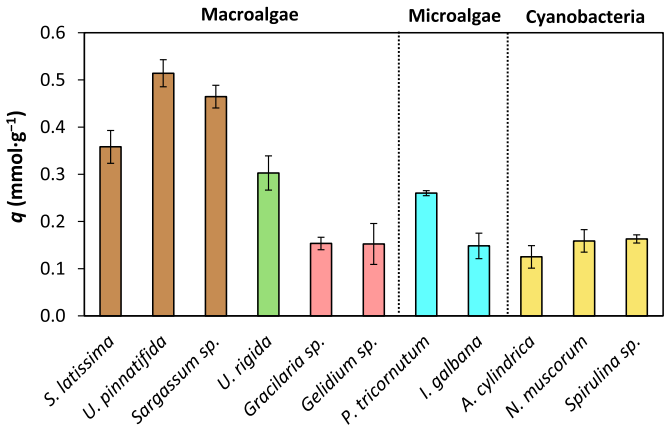

Fig. 1. Metal sorption capacity (q, mmol·g^{-1}) of each biomass at a total metal concentration of 40 ppm, 500 ppm of biomass, T = (303 ± 1) K, pH = 4 and t = 6 h. Colors were used to differentiate the biomass samples: brown bars for brown macroalgae, green bars for green macroalgae, pink bars for red macroalgae, blue bars for microalgae and yellow bars for cyanobacteria. (For interpretation of the references to color in this figure legend, the reader is referred to the Web version of this article.)

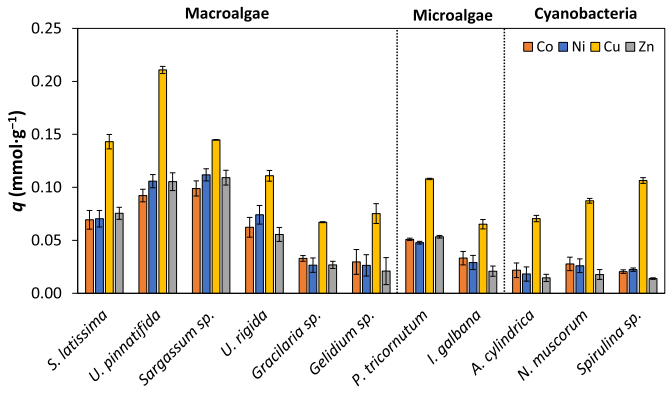

Fig. 2. Metal sorption capacity (q, mmol·g^{-1}) of each biomass for Co^{2+} (orange bars), Ni^{2+} (blue bars), Cu^{2+} (yellow bars) and Zn^{2+} (grey bars). (For interpretation of the references to color in this figure legend, the reader is referred to the Web version of this article.)

Cu^{2+}, Ni^{2+} and Zn^{2+}. Overall, the metal sorption trend was the same as observed here: *Sargassum* sp. > *Ulva* sp. > *Gracilaria* sp. The maximum sorption capacity obtained in this mono-elemental assay is significantly higher than those obtained here. This highlights that the presence of multiple ions in solution promotes intra-system competition and lowers the sorption capacity. Hence, mono-elemental studies do not reflect the real biomass potential for metal sorption in more complex matrices, as wastewaters. As for microalgae, *P. tricornutum* afforded more promising results than *I. galbana*, with its total sorption capacity being similar to that of the green macroalgal *U. rigida.* To the best of our knowledge, there are no reports employing the non-living *P. tricornutum* and *I. galbana* for metal sorption in either mono- or multi-elemental studies. The different sorption capacity of these two microalgae may rely on their structural differences. *P. tricornutum* is a diatom and, therefore, has a silica frustule rich in silanol groups, hydroxyl and carboxyl groups (Kiran Marella et al., 2020). Although no silanol groups were identified in the FTIR spectrum of *P. tricornutum,* its corresponding peaks may be overlapping with other functional groups. Regarding cyanobacteria, their sorption capacity was comparable to that of the red macroalgae and the microalgae *I. galbana*. Mono-elemental studies involving *Anabaena* sp., *Nostoc* sp. and *Spirulina platensis* (Corder and Reeves, 1994; Çelekli and Bozkurt, 2011). afforded higher sorption capacity values than those obtained herein. Overall, our results reinforce the need to evolve from mono-to multi-elemental studies and enable the establishment of a trend for the biomass sorption capacity that seems to be as follows: cyanobacteria < microalgae < macroalgae.

Despite having different metal sorption capacities, all the evaluated biomass samples display a selective metal sorption behavior, as depicted in Fig. 2.

All the studied biomass samples showed a higher affinity for Cu^{2+} than for the remaining metals. No other consistent sorption pattern could be identified across all the biomass samples for Co^{2+}, Ni^{2+} and Zn^{2+}. Although cyanobacteria were the least effective biosorbent, they displayed the highest relative Cu^{2+} selectivity (see Fig. S2). The affinity for Cu^{2+} is likely related to the complexation constant of these metals with the functional groups relevant to sorption. For instance, in the case of a simple carboxylic acid like acetic acid, the logarithm of the complexation constant values for each metal at 298 K and 0 ionic strength is as follows: 1.5 Co^{2+}, 2.2 Cu^{2+}, 1.4 Ni^{2+} and 1.6 Zn^{2+} (see Table S1). (Martell and Smith, 1977) The metal ion Cu^{2+} presents a higher complexation constant value than the remaining evaluated metals and, as a consequence, it is preferentially sorbed. The remaining metals share similar complexation constants, which leads to their indiscriminate sorption onto the biomass. The greater complexation constant value of Cu^{2+}, in comparison to Co^{2+}, Ni^{2+} and Zn^{2+}, is also verified for the hydroxide ion (Smith and Martell, 1975) and most amino acids (Martell and Smith, 1974). The preferential removal of Cu^{2+} over Co^{2+}, Ni^{2+} and Zn^{2+} was reported in other studies (Romera et al., 2007; Sheng et al., 2004), including in multi-elemental sorption assays performed in acid mine drainage (Ramasamy et al., 2019). The Cu^{2+} selectivity is also in agreement with the Irving-Williams series (Irving and Williams, 1948, 1953). The Irving-Williams series describes the relative stability order of octahedral complexes formed by M^{2+} first-row transition metal, irrespective of the ligand. The stability order of these complexes for the replacement of water by other ligands is as follows: $Mn^{2+} < Fe^{2+} < Co^{2+} < Ni^{2+} < Cu^{2+} > Zn^{2+}$ (Irving and Williams, 1948, 1953). These findings are mainly related to the ionic radius of the elements and the crystal field stabilization energy. The higher stability of the octahedral Cu^{2+} complex represents an exception to this due to the Jahn–Teller effect. Briefly, in the case of Cu^{2+}, there is an uneven distribution of electrons in the e_g set of orbitals, enabling the possibility to asymmetrically fill the orbitals. This is followed by Jahn–Teller distortion, which causes a tetragonal elongation and the stabilization of the complex (Köppel et al., 2010). This comparison is facilitated due to the uniform valency of the studied metals (M^{2+}). Sorption assays involving metals with different valency will probably impact the trends presented in this work.

3.2. Biomass characterization and sorption mechanism

The carbon, hydrogen, nitrogen, sulfur, oxygen, ash content (%) and carbon/oxygen ratio (C/O) of the screened biomass is presented in Table 1.

Overall, all biomass samples display high carbon and oxygen content but low hydrogen, nitrogen and sulfur percent. The ash content ranged from 3 to 37% with macroalgae generally having a higher ash percent than microalgae and cyanobacteria. Macroalgae exhibited low nitrogen content, which could be a reflection of their overall poor protein content, as reported elsewhere (Peñalver et al., 2020). In addition, macroalgae display lower C/O ratio values than microalgae and cyanobacteria. Brown macroalgae (*S. latissima*, *U. pinnatifida* and *Sargassum* sp.) afforded the lowest C/O ratio values, which can be linked to their high alginic acid content and low lipid abundance (Davis et al., 2003; Peñalver et al., 2020). Both the green (*U. rigida*) and red macroalgae (*Gracilaria* sp. and *Gelidium* sp.) have higher sulfur content than the remaining samples. In the case of red macroalgae, this is likely related to the abundance of sulfated galactan in their structure.

The biomass elemental composition was plotted against its sorption

Table 1
Carbon, hydrogen, nitrogen, sulfur, oxygen, ash content (%) and C/O ratio of the non-living dry biomass.

	Biomass	% C ± σ	% H ± σ	% N ± σ	% S ± σ	% ash	% O	C/O ratio
Macroalgae	*S. latissima*	26.2 ± 0.1	4.3 ± 0.1	3.94 ± 0.04	0.8 ± 0.4	36	29	0.9
	U. pinnatifida	29.1 ± 0.1	4.68 ± 0.02	2.63 ± 0.03	0.8 ± 0.4	37	25	1.1
	Sargassum sp.	37.3 ± 0.2	5.0 ± 0.1	1.3 ± 0.1	0.5 ± 0.1	17	39	1.0
	U. rigida	30.10 ± 0.01	5.1 ± 0.1	3.78 ± 0.08	5.1 ± 0.7	32	24	1.3
	Gracilaria sp.	32.9 ± 0.2	4.92 ± 0.08	3.41 ± 0.07	2.0 ± 0.1	27	30	1.1
	Gelidium sp.	38.3 ± 0.1	5.85 ± 0.06	3.06 ± 0.07	1.9 ± 0.3	16	35	1.1
Microalgae	*P. tricornutum*	41.3 ± 0.2	5.9 ± 0.2	6.22 ± 0.04	0.8 ± 0.2	19	26	1.6
	I. galbana	48.42 ± 0.03	6.63 ± 0.06	7.770 ± 0.004	0.7 ± 0.1	13	24	2.0
Cyanobacteria	*A. cylindrica*	45.0 ± 0.2	6.4 ± 0.3	7.64 ± 0.04	0 ± 0	4	37	1.2
	N. muscorum	49.4 ± 0.1	6.81 ± 0.01	10.97 ± 0.05	0.19 ± 0.03	3	29	1.7
	Spirulina sp.	48.9 ± 0.4	6.57 ± 0.07	11.1 ± 0.3	0.55 ± 0.04	7	25	1.9

capacity (q, mmol·g^{-1}) to study a potential correlation between these parameters (Fig. 3). Red macroalgae (*Gracilaria* sp. and *Gelidium* sp.) were excluded from this evaluation as they do not follow the trends observed for the other biomass samples.

The data suggest a strong correlation between carbon, nitrogen and hydrogen content and the metal sorption capacity. On the other hand, the sulfur and oxygen biomass content do not seem to be associated with the sorption capacity of the biomass. The plot of C/O ratio *versus* metal sorption capacity seems to suggest that higher C/O ratios are linked to lower sorption capacity values. Still, this dependency is weak and more data would be required to validate this observation. In this work ground non-living biomass was used in all assays. For this reason, there is no distinction between intracellular or surface groups, with all functional groups being available to interact with metal. Establishing these correlations in living biomass is not valid since not all elements will be available for metal interaction, depending on their location.

The sorption of metals highly depends on the functional groups present in each biomass sample. FTIR was used to identify the main functional groups of each biomass and details are presented in Tables 2 and 3. Spectra details can be consulted in Figs. S3 and S4.

According to the FTIR spectra, all the evaluated biomass samples presented O–H and N–H stretching vibrations around 3208 and 3296 cm^{-1}, C═O stretching vibration from the amide I band at 1610–1644 cm^{-1} and N–H stretching vibration of the amide II band at 1538–1542 cm^{-1}. The FTIR spectra of *Sargassum* sp. showed some changes after contact with the multi-elemental metal solution. For instance, the peak

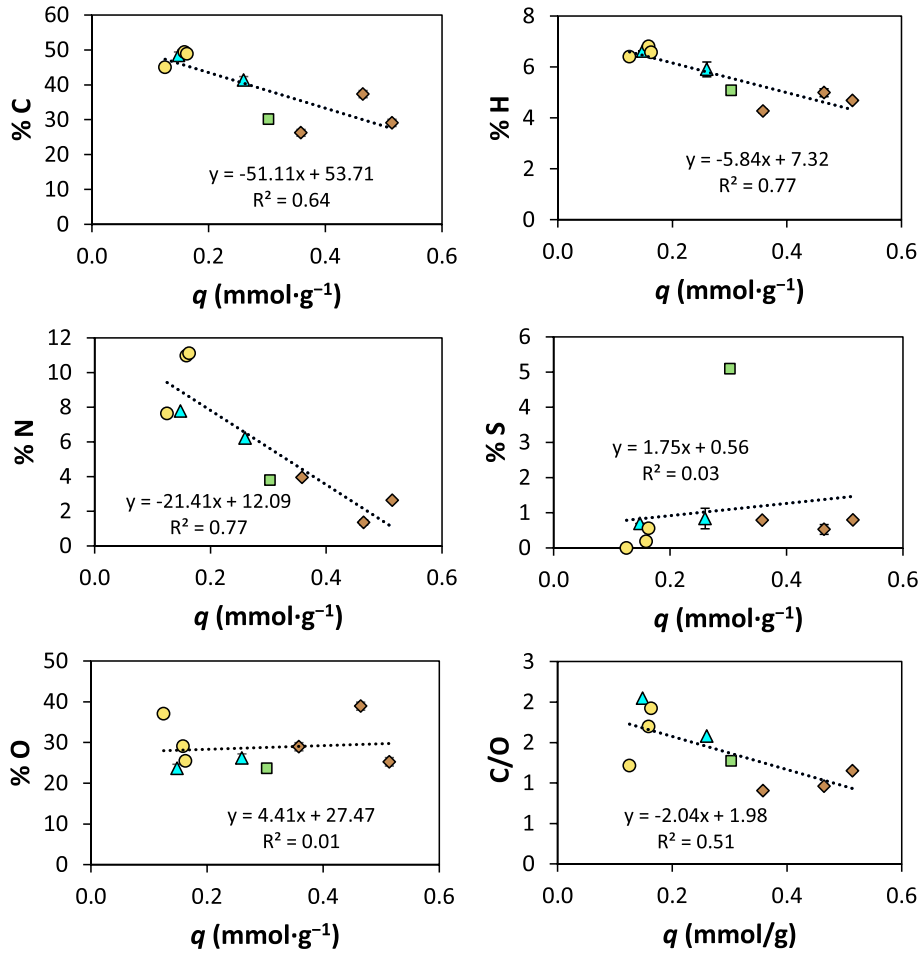

Fig. 3. Correlation between carbon, hydrogen, nitrogen, sulfur, oxygen, ash content (%) and carbon/oxygen ratio with the sorption capacity (q, mmol·g^{-1}) of the screened biomass. Each color represents a set of organisms, brown (◊) corresponding to brown macroalgae, green (□) to green macroalgae, blue (Δ) to microalgae and yellow (○) to cyanobacteria. (For interpretation of the references to color in this figure legend, the reader is referred to the Web version of this article.)

Table 2
Identification of the main FTIR bands of the studied macroalgae before metal sorption.

Band origin	Wavenumber (cm^{-1})					
	S. latissima	*U. pinnatifida*	*Sargassum* sp.	*U. rigida*	*Gracilaria* sp.	*Gelidium* sp.
ν O–H (polysaccharides), ν N–H (proteins)	3269	3285	3278	3208	3296	3354
ν C–H of aliphatic groups	2934	2925	2925	2950	2924, 2871	2927
ν C═O (amide I band)	1633	1622	1610	1633	1644	1633
δ N–H (amide II band)	1538	1538	1542	1548	1538	1548
δ O–H (carboxyl and hydroxyl groups)	1416	1416	1420	1404	1416	1415
δ C–H, δ O–H, (III amide band, proteins)	–	1241	1213	1227	–	–
ν C–O (aliphatic ether, primary and secondary alcohol)	1081, 1021	1028	1161, 1028	1149, 1082	1035	1149, 1035
ν C–O	931	–	–	–	930	931

Table 3
Identification of the main FTIR bands of the studied microalgae and cyanobacteria before metal sorption.

Band origin	Wavenumber (cm^{-1})				
	Microalgae		Cyanobacteria		
	P. tricornutum	*I. galbana*	*A. cylindrica*	*N. muscorum*	*Spirulina* sp.
ν O–H (polysaccharides), ν N–H (proteins)	3280	3274	3280	3282	3280
ν C–H of aliphatic groups	2959, 2923, 2852	2957, 2919, 2849	2957, 2926, 2894, 2856	2923, 2875, 2852	2926, 2874, 2856
ν C═O (amide I band)	1633	1633	1644	1634	1634
δ N–H (amide II band)	1538	1538	1538	1538	1538
δ C–H (methyl and methylene groups)	1469	1454	1454	1454	1454
δ O–H (carboxyl and hydroxyl groups)	1402	1403	1393	1393	1393
δ C–H, δ O–H, (III amide band, proteins)	1227	1234	1241	1240	1239
ν C–O (aliphatic ether, primary and secondary alcohol)	1039	1103, 1072, 1040	1151, 1078, 1022	1152, 1045	1030

at 1321 cm^{-1} corresponding to the C–O stretching vibration disappeared upon contact with the metal solution. There are also modifications around 1416 cm^{-1}, suggesting the involvement of carboxyl groups. In the case of *P. tricornutum*, there are modifications in the amide II band region (≈1542 cm^{-1}), corresponding to N–H bending vibrations. This macroalgae also presents modifications around 1402 cm^{-1}, corresponding to carboxyl and hydroxyl bending vibrations and modifications around 1469 cm^{-1} corresponding to methyl and methylene bending vibrations. *Spirulina* sp. showed no significant alterations before and after metal sorption. Among these three biomass samples, *Spirulina* sp. was the least efficient metal sorbent. The amount of metal sorbed to its cell wall may not be enough to afford visible changes in the FTIR analysis. Of the identified functional groups, the carboxyl groups seem to be significantly involved in metal sorption. At pH = 4 most carboxyl groups are deprotonated (pK_a 1.7–4.7) and, therefore, available for metal sorption (Dean, 1999). Despite the importance of the carboxyl groups for metal sorption, according to the oxygen percent and sorption capacity correlation, the oxygen content alone does not seem to be directly related to the sorption capacity of the biomass, as shown in Fig. 1. In this case, the availability of the right type of oxygen-containing functional groups to interact with metals may be more important than their abundance.

Since ion-exchange is one of the potential mechanisms behind metal sorption (Michalak et al., 2018), the inorganic components of the biomass samples were quantified *via* TXRF and are presented in Table S2. The evaluated biomass samples have significant concentrations of Cl^-, K^+ and Ca^{2+} (Fig. S5). TXRF is not the most suitable equipment for anion quantification so the presented Cl^- concentration may not be accurate. The abundance of K^+ and Ca^{2+} is particularly relevant from an ion-exchange point of view. Other ions such as Na^+ and Mg^{2+} are also expected to be in the biomass structure but their quantification is not feasible in TXRF. These ions are generally coordinated with the acidic functional groups of the biomass and can be exchanged by other cations present in the solution. The abundance and diversity of ions in the biomass structure are influenced by the environment where they are grown. For instance, the lab-grown cyanobacteria *A. cylindrica* and *N. muscorum* may display significantly lower amounts of these inorganic ions due to the controlled environment they were grown in. No obvious correlation was found between the K^+ and Ca^{2+} concentration on the biomass and its sorption capacity.

Considering that, as discussed above, some metal complexes are more stable than others, it is likely that under appropriate conditions a metal can displace another ion from a less stable complex (Irving and Williams, 1948). To better understand the sorption mechanism, besides the Ca^{2+} and K^+ concentrations present on the biomass samples detailed in Table S2, the Ca^{2+} and K^+ concentrations were measured for all the controls and samples. While the controls showed no traces of these ions, a significant release of Ca^{2+} and K^+ from the biomass to the multi-elemental metal solution was observed in all biomass samples upon metal sorption. The release of these ions was quantified *via* TXRF for all assays and is depicted in Fig. S6. The correlation between the release of Ca^{2+} and K^+ ions and metal sorption is presented in Fig. 4. As in the elemental composition vs q correlation, red macroalgae (*Gracilaria* sp. and *Gelidium* sp.) were excluded from the analyses as they have a behavior clearly different from the other biomass samples studied. The cyanobacterium *P. tricornutum* was also excluded, but only from the Ca^{2+} release vs q correlation, as it significantly impaired the trend (R^2 drop from 0.61 to 0.11).

The K^+ release seem to be linked to a large extent to the metal loading into the biomass with 2 ions being removed to allow the sorption of a metal ion, as expected from electroneutrality. Although much weaker, the release of Ca^{2+} also seems to contribute to metal sorption. The total amount of released K^+ and Ca^{2+} was charge normalized and compared to the amount of sorbed metals (see Fig. S7). Overall, the amount of released ions is very similar to the amount of sorbed metals when considering charge normalization. The only exception is *U. pinnatifida*, where the sum of normalized K^+ and Ca^{2+} exceeds the amount of sorbed metals. Since K^+ and Ca^{2+} largely account for all sorbed metals, other ions as Mg^{2+} and Na^+ are unlikely to be involved in the described sorption mechanism. The displacement of these ions confirms the involvement of the ion-exchange mechanism in multi-elemental metal sorption assays. The replacement of the Ca^{2+} and K^+ ions can be further related to their complexation constants with the biomass functional groups. According to the complexation constant values of Ca^{2+}, K^+, Co^{2+}, Cu^{2+}, Ni^{2+} and Zn^{2+} with the hydroxide ion and carboxylic acids (oxalic and citric acid) (Martell and Smith, 1977;

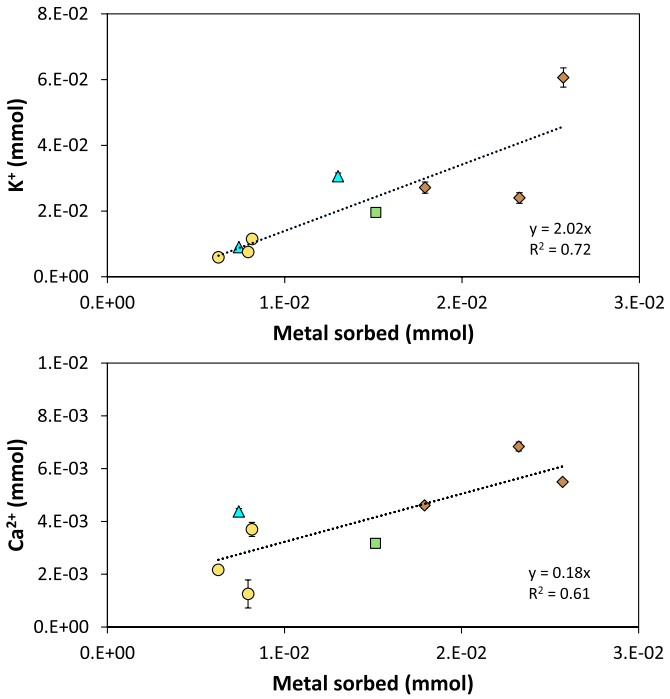

Fig. 4. Correlation of the K^+ and Ca^{2+} release with the metal sorbed (mmol) for the different biomass samples. Colors were used to differentiate the biomass: brown (◊) for brown macroalgae, green (□) for green macroalgae, blue (Δ) for microalgae and yellow (○) for cyanobacteria. The linear regression is represented by the black dotted line. (For interpretation of the references to color in this figure legend, the reader is referred to the Web version of this article.)

Smith and Martell, 1975), Ca^{2+} and K^+ typically have lower complexation constants than the evaluated transition metals. In the case of the hydroxide ion, the logarithm of the complexation constant values for each metal at 298 K and 0 ionic strength is as follows: 1.3 Ca^{2+}, −0.5 K^+, 4.3 Co^{2+}, 6.3 Cu^{2+}, 4.1 Ni^{2+} and 5.0 Zn^{2+} (Table S1). When compared to Ca^{2+}, K^+ has a lower complexation constant. Consequently, K^+ should be more easily exchanged with metal ions than Ca^{2+}. This is supported by the obtained data since K^+ ions were more extensively released from the biomass to the aqueous solution than Ca^{2+} ions (see Fig. 4). The red algae always diverge from the presented correlations, suggesting that their metal sorption mechanism may differ from that described for the remaining biomass samples.

4. Conclusions

Eleven non-living algal biomass samples were screened for metal sorption in multi-elemental metal solutions containing equal concentrations of Co^{2+}, Cu^{2+}, Ni^{2+} and Zn^{2+} at (303 ± 1) K and pH = 4. The composition of the biomass was found to be correlated with their sorption capacity. According to the FTIR spectra of the biomass, carboxyl groups are involved in metal sorption. Despite the strong involvement of oxygen-rich groups in metal sorption, higher biomass oxygen contents do not correlate with better metal sorption capacity values, suggesting that the type, distribution and accessibility of the functional groups are more important than their abundance. Brown macroalgae afforded higher metal sorption capacity values than the remaining evaluated biomass samples. Regardless of being macroalgae, microalgae or cyanobacteria, all biomasses showed a higher affinity for Cu^{2+} sorption. To shed light on the metal sorption mechanism in multi-elemental assays, the release of Ca^{2+} and K^+ to the aqueous media was investigated. The obtained results suggest that the release of these ions, in particular K^+, is linked to the metal sorption capacity values. This indicates that for most of the studied biomass types, ion-exchange is the prevalent mechanism involved in metal sorption. Altogether, using biomass as a pre-concentrator can be a viable vessel for metal recovery from multi-elemental metal solutions.

Credit author statement

Ana R. F. Carreira: Investigation, Visualization, Writing – original draft; **Telma Veloso**: Investigation, Visualization, Writing – review & editing; **Inês P. E. Macário**: Investigation, Visualization, Writing – review & editing; **Joana L. Pereira**: Conceptualization, Writing – review & editing.**Sónia P. M. Ventura**: Conceptualization, Funding acquisition, Writing – review & editing **Helena Passos**: Conceptualization, Visualization, Supervision, Writing – review & editing; **João A. P. Coutinho**: Conceptualization, Supervision, Writing – review & editing.

Declaration of competing interest

The authors declare that they have no known competing financial interests or personal relationships that could have appeared to influence the work reported in this paper.

Data availability

Data will be made available on request.

Acknowledgments

This work was developed within the scope of the project CICECO-Aveiro Institute of Materials, UIDB/50011/2020, UIDP/50011/2020 & LA/P/0006/2020, financed by national funds through the FCT/MEC (PIDDAC) and CESAM (UIDP/50017/2020+UIDB/50017/2020+LA/P/0094/2020). Ana R. F. Carreira, Telma Veloso and Inês P. E. Macário acknowledge FCT for the Ph.D. grants SFRH/BD/143612/2019, SFRH/BD/147346/2019 and SFRH/BD/123850/2016, respectively. Helena Passos acknowledges FCT – Fundação para a Ciência e a Tecnologia, I.P. for the researcher contract CEECIND/00831/2017 under the Scientific Employment Stimulus - Individual Call 2017. The authors acknowledge the financial support of FCT regarding the project REFINECYANO (PTDC/BTA-BTA/30914/2017). The authors would like to thank Nicolas Schaeffer (CICECO) for fruitful discussions and ALGAplus, Lda. for providing algal samples.

Appendix A. Supplementary data

Supplementary data to this article can be found online at https://doi.org/10.1016/j.chemosphere.2022.137675.

References

Ajjabi, L.C., Chouba, L., 2009. Biosorption of Cu2+ and Zn2+ from aqueous solutions by dried marine green macroalga Chaetomorpha linum. J. Environ. Manag. 90, 3485–3489. https://doi.org/10.1016/j.jenvman.2009.06.001.

Akpomie, K.G., Dawodu, F.A., Adebowale, K.O., 2015. Mechanism on the sorption of heavy metals from binary-solution by a low cost montmorillonite and its desorption potential. Alex. Eng. J. 54, 757–767. https://doi.org/10.1016/j.aej.2015.03.025.

Bina, B., Kermani, M., Movahedian, H., Khazaei, Z., 2006. Biosorption and recovery of copper and zinc from aqueous solutions by nonliving biomass of marine brown algae of Sargassum sp. Pakistan J. Biol. Sci. 9, 1525–1530. https://doi.org/10.3923/pjbs.2006.1525.1530.

Birloaga, I., Vegliò, F., 2022. An innovative hybrid hydrometallurgical approach for precious metals recovery from secondary resources. J. Environ. Manag. 307, 114567 https://doi.org/10.1016/j.jenvman.2022.114567.

Blanco Vieites, M., Suarez Montes, D., Delgado, F., Álvarez-Gil, M., Battez, A.H., Rodriguez, E., 2022. Removal of heavy metals and hydrocarbons by microalgae from wastewater in the steel industry. Algal Res. 64, 102700 https://doi.org/10.1016/j.algal.2022.102700.

Çelekli, A., Bozkurt, H., 2011. Bio-sorption of cadmium and nickel ions using Spirulina platensis: kinetic and equilibrium studies. Desalination 275, 141–147. https://doi.org/10.1016/j.desal.2011.02.043.

Christmann, P., Lefebvre, G., 2022. Trends in global mineral and metal criticality: the need for technological foresight. Miner. Econ. 1, 1–12. https://doi.org/10.1007/s13563-022-00323-5.
Corder, S.L., Reeves, M., 1994. Biosorption of nickel in complex aqueous waste streams by cyanobacteria. Appl. Biochem. Biotechnol. 45–46, 847–859. https://doi.org/10.1007/BF02941854.
Costa, M., Henriques, B., Pinto, J., Fabre, E., Dias, M., Soares, J., Carvalho, L., Vale, C., Pinheiro-Torres, J., Pereira, E., 2020. Influence of toxic elements on the simultaneous uptake of rare earth elements from contaminated waters by estuarine macroalgae. Chemosphere 252, 126562. https://doi.org/10.1016/j.chemosphere.2020.126562.
Davis, T.A., Volesky, B., Mucci, A., 2003. A review of the biochemistry of heavy metal biosorption by brown algae. Water Res. 37, 4311–4330. https://doi.org/10.1016/S0043-1354(03)00293-8.
Dean, J.A., 1999. Lange's Handbook of Chemistry, fifteenth ed. McGraw-Hill, Inc.
Dodbiba, G., Ponou, J., Fujita, T., 2015. Biosorption of heavy metals. In: Microbiol. Miner. Met. Mater. Environ., pp. 409–426. https://doi.org/10.4018/978-1-5225-8903-7.ch077
Dolker, T., Pant, D., 2019. Chemical-biological hybrid systems for the metal recovery from waste lithium ion battery. J. Environ. Manag. 248, 109270 https://doi.org/10.1016/j.jenvman.2019.109270.
Dutta, D., Arya, S., Kumar, S., 2021. Industrial wastewater treatment: current trends, bottlenecks, and best practices. Chemosphere 285, 131245. https://doi.org/10.1016/j.chemosphere.2021.131245.
Escudero Onate, C., Villaescusa, I., 2018. The Thermodynamics of Heavy Metal Sorption onto Lignocellulosic Biomass. Heavy Met. https://doi.org/10.5772/intechopen.74260.
Fabre, E., Henriques, B., Viana, T., Pinto, J., Costa, M., Ferreira, N., Tavares, D., Vale, C., Pinheiro-Torres, J., Pereira, E., 2021. Optimization of Nd(III) removal from water by Ulva sp. and Gracilaria sp. through response surface methodology. J. Environ. Chem. Eng. 9, 105946 https://doi.org/10.1016/j.jece.2021.105946.
Gahlout, M., prajapati, H., Chauhan, P., Savande, L., Yadav, P., 2017. Isolation, screening and identification of cyanobacteria and its uses in bioremediation of industrial effluents and chromium sorption. Int. J. Adv. Res. Biol. Sci. 4, 138–146. https://doi.org/10.22192/IJARBS.2017.04.04.019.
Ibrahim, W.M., Abdel Aziz, Y.S., Hamdy, S.M., Gad, N.S., 2018. Comparative study for biosorption of heavy metals from synthetic wastewater by different types of marine algae. J. Biorem. Biodegrad. 1–7. https://doi.org/10.4172/2155-6199.1000425, 09.
Inthorn, D., Sidtitoon, N., Silapanuntakul, S., Incharoensakdi, A., 2002. Sorption of mercury , cadmium and lead by microalgae. Sci. Asia 28, 253–261.
Irving, H., Williams, R.J.P., 1948. Order of stability of metal complexes. Nat 162, 746–747. https://doi.org/10.1038/162746a0, 1948 1624123.
Irving, H., Williams, R.J.P., 1953. The stability of transition-metal complexes. J. Chem. Soc. 3192–3210. https://doi.org/10.1039/JR9530003192.
Javanbakht, V., Alavi, S.A., Zilouei, H., 2014. Mechanisms of heavy metal removal using microorganisms as biosorbent. Water Sci. Technol. 69, 1775–1787. https://doi.org/10.2166/wst.2013.718.
Kamarudzaman, A.N., Ain Che Adan, S.N., Hassan, Z., Ab Wahab, M., Zaini Makhtar, S. M., Abu Seman, N.A., Ab Jalil, M.F., Handayani, D., Syafiuddin, A., 2022. Biosorption of copper(Ii) and iron(ii) using spent mushroom compost as biosorbent. Biointerface Res. Appl. Chem. 12, 7775–7786. https://doi.org/10.33263/BRIAC126.77757786.
Kanamarlapudi, S.L.R.K., Chintalpudi, V.K., Muddada, S., 2018. Application of Biosorption for Removal of Heavy Metals from Wastewater. Biosorption. https://doi.org/10.5772/intechopen.77315.
Kayranli, B., Gok, O., Yilmaz, T., Gok, G., Celebi, H., Seckin, I.Y., Mesutoglu, O.C., 2022. Low-cost organic adsorbent usage for removing Ni2+ and Pb2+ from aqueous solution and adsorption mechanisms. Int. J. Environ. Sci. Technol. 19, 3547–3564. https://doi.org/10.1007/s13762-021-03653-z.
Kiran Marella, T., Saxena, A., Tiwari, A., 2020. Diatom mediated heavy metal remediation: a review. Bioresour. Technol. 305, 123068 https://doi.org/10.1016/j.biortech.2020.123068.
Koppel, H., Yarkony, D.R., Barentzen, H., 2010. The Jahn - teller effect - fundamentals and implications for physics and chemistry. Springer Chem. Phys. 97, 912. http://link.springer.com/10.1007/978-3-642-03432-9.
Li, P., feng Cai, M., 2021. Challenges and new insights for exploitation of deep underground metal mineral resources. Trans. Nonferrous Met. Soc. China (English Ed. 31, 3478–3505. https://doi.org/10.1016/S1003-6326(21)65744-8.
Lin, Z., Li, J., Luan, Y., Dai, W., 2020. Application of algae for heavy metal adsorption: a 20-year meta-analysis. Ecotoxicol. Environ. Saf. 190, 110089 https://doi.org/10.1016/j.ecoenv.2019.110089.
Martell, A.E., Smith, R.M., 1974. Critical Stability Constants: Amino Acids. Plenum Press, New York; London.
Martell, A.E., Smith, R.M., 1977. Other Organic Ligands, first ed. Springer, New York, NY. https://doi.org/10.1007/978-1-4757-1568-2.
Michalak, I., Mironiuk, M., Marycz, K., 2018. A comprehensive analysis of biosorption of metal ions by macroalgae using ICP-OES, SEM-EDX and FTIR techniques. PLoS One 13. https://doi.org/10.1371/journal.pone.0205590.
Millan Becerro, R., Macías, F., Cánovas, C.R., Pérez López, R., Fuentes López, J.M., 2022. Environmental management and potential valorization of wastes generated in passive treatments of fertilizer industry effluents. Chemosphere 295, 133876. https://doi.org/10.1016/j.chemosphere.2022.133876.
Miyamoto, W., Kosai, S., Hashimoto, S., 2019. Evaluating metal criticality for low-carbon power generation technologies in Japan. Minerals 9, 95. https://doi.org/10.3390/min9020095.
Nobahar, A., Melka, A.B., Pusta, A., Lourenço, J.P., Carlier, J.D., Costa, M.C., 2022. A new application of solvent extraction to separate copper from extreme acid mine drainage producing solutions for electrochemical and biological recovery processes. Mine Water Environ. 41, 387–401. https://doi.org/10.1007/S10230-022-00858-7/FIGURES/9.
Peñalver, R., Lorenzo, J.M., Ros, G., Amarowicz, R., Pateiro, M., Nieto, G., 2020. Seaweeds as a functional ingredient for a healthy diet. Mar. Drugs 18. https://doi.org/10.3390/md18060301.
Pennesi, C., Totti, C., Romagnoli, T., Bianco, B., De Michelis, I., Beolchini, F., 2012. Marine macrophytes as effective lead biosorbents. Water Environ. Res. 84, 9–16. https://doi.org/10.2175/106143011x12989211841296.
Piccini, M., Raikova, S., Allen, M.J., Chuck, C.J., 2018. A synergistic use of microalgae and macroalgae for heavy metal bioremediation and bioenergy production through hydrothermal liquefaction. Sustain. Energy Fuels 3, 292–301. https://doi.org/10.1039/C8SE00408K.
Radway, J.A.C., Wilde, E.W., Whitaker, M.J., Weissman, J.C., 2001. Screening of algal strains for metal removal capabilities. J. Appl. Phycol. 13, 451–455. https://doi.org/10.1023/A:1011111711821.
Ramasamy, D.L., Porada, S., Sillanpää, M., 2019. Marine algae: a promising resource for the selective recovery of scandium and rare earth elements from aqueous systems. Chem. Eng. J. 371, 759–768. https://doi.org/10.1016/j.cej.2019.04.106.
Romera, E., González, F., Ballester, A., Blázquez, M.L., Muñoz, J.A., 2007. Comparative study of biosorption of heavy metals using different types of algae. Bioresour. Technol. 98, 3344–3353. https://doi.org/10.1016/j.biortech.2006.09.026.
Salam, K.A., 2019. Towards sustainable development of microalgal biosorption for treating effluents containing heavy metals. Biofuel Res. J. 6, 948–961. https://doi.org/10.18331/BRJ2019.6.2.2.
Shaaban, A.E.S.M., Badawy, R.K., Mansour, H.A., Abdel-Rahman, M.E., Aboulsoud, Y.I. E., 2017. Competitive algal biosorption of Al3+, Fe3+, and Zn2+ and treatment application of some industrial effluents from Borg El-Arab region, Egypt. J. Appl. Phycol. 29, 3221–3234. https://doi.org/10.1007/s10811-017-1185-4.
Sheikh, Z., Amin, M., Khan, N., Khan, M.N., Sami, S.K., Khan, S.B., Hafeez, I., Khan, S.A., Bakhsh, E.M., Cheng, C.K., 2021. Potential application of Allium Cepa seeds as a novel biosorbent for efficient biosorption of heavy metals ions from aqueous solution. Chemosphere 279, 130545. https://doi.org/10.1016/j.chemosphere.2021.130545.
Sheng, P.X., Ting, Y.P., Chen, J.P., Hong, L., 2004. Sorption of lead, copper, cadmium, zinc, and nickel by marine algal biomass: characterization of biosorptive capacity and investigation of mechanisms. J. Colloid Interface Sci. 275, 131–141. https://doi.org/10.1016/j.jcis.2004.01.036.
Smith, R.M., Martell, A.E., 1975. Critical Stability Constants: Inorganic Complexes. https://doi.org/10.1007/978-1-4613-4452-0.
thi Quyen, V., Pham, T.H., Kim, J., Thanh, D.M., Thang, P.Q., Van Le, Q., Jung, S.H., Kim, T.Y., 2021. Biosorbent derived from coffee husk for efficient removal of toxic heavy metals from wastewater. Chemosphere 284, 131312. https://doi.org/10.1016/j.chemosphere.2021.131312.
Wang, J., Chen, C., 2009. Biosorbents for heavy metals removal and their future. Biotechnol. Adv. 27, 195–226. https://doi.org/10.1016/j.biotechadv.2008.11.002.
Wang, Q., Wang, Y., Tang, J., Yang, Z., Zhang, L., Huang, X., 2022. New insights into the interactions between Pb(II) and fruit waste biosorbent. Chemosphere 303, 135048. https://doi.org/10.1016/j.chemosphere.2022.135048.
Watari, T., Nansai, K., Nakajima, K., 2020. Review of critical metal dynamics to 2050 for 48 elements. Resour. Conserv. Recycl. 155, 104669 https://doi.org/10.1016/j.resconrec.2019.104669.
Womersley, H.B.S., 1973. Handbook of Phycological Methods. Culture Methods and Growth Measurements. Cambridge University Press. https://doi.org/10.1016/0304-3770(81)90012-7.
Yadav, A.P.S., Dwivedi, V., Kumar, S., Kushwaha, A., Goswami, L., Reddy, B.S., 2021. Cyanobacterial extracellular polymeric substances for heavy metal removal: a mini review. J. Compos. Sci. 5, 1. https://doi.org/10.3390/jcs5010001.
Zeraatkar, A.K., Ahmadzadeh, H., Talebi, A.F., Moheimani, N.R., McHenry, M.P., 2016. Potential use of algae for heavy metal bioremediation, a critical review. J. Environ. Manag. 181, 817–831. https://doi.org/10.1016/j.jenvman.2016.06.059.
Znad, H., Awual, M.R., Martini, S., 2022. The utilization of algae and seaweed biomass for bioremediation of heavy metal-contaminated wastewater. Molecules 27, 1275. https://doi.org/10.3390/molecules27041275.